APPLIED AND ENVIRONMENTAL MICROBIOLOGY, Dec. 2004, p. 7277–7287 Vol. 70, No. 12
0099-2240/04/$08.00+0 DOI: 10.1128/AEM.70.12.7277–7287.2004

Metabolic Fluxes in *Corynebacterium glutamicum* during Lysine Production with Sucrose as Carbon Source

Christoph Wittmann,[1]* Patrick Kiefer,[1] and Oskar Zelder[2]

Biochemical Engineering, Saarland University, Saarbrücken,[1] and Research on Fine Chemicals and Biotechnology, BASF AG, Ludwigshafen,[2] Germany

Received 5 May 2004/Accepted 22 July 2004

Metabolic fluxes in the central metabolism were determined for lysine-producing *Corynebacterium glutamicum* ATCC 21526 with sucrose as a carbon source, providing an insight into molasses-based industrial production processes with this organism. For this purpose, ^{13}C metabolic flux analysis with parallel studies on [1-$^{13}C^{Fru}$]sucrose, [1-$^{13}C^{Glc}$]sucrose, and [$^{13}C_6^{Fru}$]sucrose was carried out. *C. glutamicum* directed 27.4% of sucrose toward extracellular lysine. The strain exhibited a relatively high flux of 55.7% (normalized to an uptake flux of hexose units of 100%) through the pentose phosphate pathway (PPP). The glucose monomer of sucrose was completely channeled into the PPP. After transient efflux, the fructose residue was mainly taken up by the fructose-specific phosphotransferase system (PTS) and entered glycolysis at the level of fructose-1,6-bisphosphate. Glucose-6-phosphate isomerase operated in the gluconeogenetic direction from fructose-6-phosphate to glucose-6-phosphate and supplied additional carbon (7.2%) from the fructose part of the substrate toward the PPP. This involved supply of fructose-6-phosphate from the fructose part of sucrose either by PTS^{Man} or by fructose-1,6-bisphosphatase. *C. glutamicum* further exhibited a high tricarboxylic acid (TCA) cycle flux of 78.2%. Isocitrate dehydrogenase therefore significantly contributed to the total NADPH supply of 190%. The demands for lysine (110%) and anabolism (32%) were lower than the supply, resulting in an apparent NADPH excess. The high TCA cycle flux and the significant secretion of dihydroxyacetone and glycerol display interesting targets to be approached by genetic engineers for optimization of the strain investigated.

Corynebacterium glutamicum has been used for the industrial production of amino acids for more than 40 years. More than 1 million tons of amino acids are produced with this microorganism per annum. Cane molasses, beet molasses, and starch hydrolysate from corn or cassava are used as the main source of carbon (8). Investigation of the metabolic properties of *C. glutamicum* has made an important contribution toward optimization of strains and production processes. Recently developed approaches for the quantification of metabolic fluxes have revealed fascinating insights into the metabolism of *C. glutamicum* and provided important knowledge for targeted strain improvement (24).

Glucose has been used as the carbon source in almost all metabolic flux studies with *C. glutamicum* (10). Only selected investigations have been based on other substrates such as lactate (2), acetate (1, 23), or fructose (4, 10). Sucrose, however, has not been studied so far, despite the fact that it is successfully used for production of lysine (11, 13), valine (12), homoserine (13), or tryptophan (7) and shows high relevance for all industrial molasses-based production processes with *C. glutamicum* (8). Sucrose uptake in *C. glutamicum* occurs via a phosphotransferase system (PTS) whereby sucrose is phosphorylated at the glucose ring into sucrose-6-phosphate, followed by invertase-catalyzed hydrolysis into glucose-6-phosphate and fructose (14). Similar mechanisms have also been reported for other microorganisms such as *Streptococcus lactis* (18), *Staphylococcus xylosus* (22), and *Clostridium acetobutylicum* (17). In contrast to these bacteria, however, *C. glutamicum* does not possess an ATP-dependent fructokinase for conversion of the liberated intracellular fructose into fructose-6-phosphate (14). In fact, in this bacterium, fructose is phosphorylated by the fructose uptake systems PTS^{Fru} and PTS^{Man}, involving transient efflux out of the cell (3). This leads to a rather complex situation of three different potential entry points of the carbon source into the metabolism.

In view of the importance of sucrose as a carbon source for *C. glutamicum*, metabolic fluxes on this substrate were quantified for a lysine-producing mutant, *C. glutamicum* ATCC 21526. For this purpose, ^{13}C tracer experiments with different substrate labelings were combined with gas chromatography-mass spectrometry (GC-MS) labeling measurement of secreted metabolites, metabolite balancing, and isotopomer modeling.

MATERIALS AND METHODS

Microorganism. *C. glutamicum* ATCC 21526 was obtained from the American Type Culture Collection (Manassas, Va.). This strain requires methionine, threonine, and leucine for growth.

Medium and cultivation. Precultures were grown in complex medium (20) containing 5 g of sucrose liter^{-1}. For agar plates, the complex medium was additionally amended with 12 g of agar liter^{-1}. For production of cells as an inoculum for the tracer experiments, a minimal medium with 1 mg of calcium panthotenate · HCl liter^{-1} was used (26). Precultivation was carried out as described previously (10) except that sucrose was used as the sole source of carbon. For precultivation, the initial sucrose concentration was 40 mM. Tracer experiments were carried out in 25-ml baffled shake flasks with 4 ml of minimal medium, which did not contain any threonine, methionine, leucine, or citrate. Three parallel studies with 20 mM [1-$^{13}C^{Fru}$]sucrose, i.e., sucrose specifically ^{13}C labeled at carbon 1 of its fructose monomer, 20 mM [1-$^{13}C^{Glc}$]sucrose, i.e., sucrose specifically ^{13}C labeled at carbon 1 of its glucose monomer, and 20 mM [$^{13}C_6^{Fru}$]sucrose, i.e., sucrose fully ^{13}C labeled at all carbons of its fructose monomer, respectively, were carried out.

* Corresponding author. Mailing address: Biochemical Engineering, Saarland University, Im Stadtwald, 66041 Saarbrücken, Germany. Phone: 49-681-302-2205. Fax: 49-681-302-4572. E-mail: c.wittmann@mx.uni-saarland.de.

TABLE 1. Biomass and metabolites in the stage of lysine production by *C. glutamicum* ATCC 21526 from sucrose

Product	Yield coefficient[a]
Biomass	54.0 ± 0.4
Lysine	549.2 ± 33.1
Alanine	1.1 ± 0.9
Glycine	15.8 ± 6.6
Dihydroxyacetone	167.7 ± 25.8
Glycerol	9.6 ± 3.2
Trehalose	5.4 ± 1.1
Acetate	60.9 ± 31.9
Pyruvate	1.1 ± 1.5
Lactate	30.4 ± 5.7

[a] Values are means from parallel incubations on 20 mM [1-$^{13}C^{Fru}$]sucrose, 20 mM [1-$^{13}C^{Glc}$]sucrose, and 20 mM [$^{13}C_6{}^{Fru}$]sucrose, with corresponding deviations between the three cultivations. All yields are expressed as millimoles of product per mole of sucrose except for the yield for biomass, which is expressed as milligrams of dry biomass per millimole of sucrose.

Chemicals. [1-$^{13}C^{Fru}$]sucrose, [1-$^{13}C^{Glc}$]sucrose, and [$^{13}C_6{}^{Fru}$]sucrose, all with 99% ^{13}C enrichment, were purchased from Campro Scientific (Veenendaal, The Netherlands). Yeast extract and tryptone were obtained from Difco Laboratories (Detroit, Mich.). All other chemicals were from Sigma (St. Louis, Mo.), Merck (Darmstadt, Germany), or Fluka (Buchs, Switzerland) and were of analytical grade.

Substrate and product analysis. Quantification of extracellular substrates and products involving sucrose, trehalose, glucose, and fructose (GC), acetate, lactate, pyruvate, and 2-oxoglutarate (high-performance liquid chromatography), glycerol and dihydroxyacetone (enzyme assay), and amino acids (high-performance liquid chromatography) was carried out as described previously (10). Cell concentrations were determined with a photometer or by gravimetric analysis as described by Wittmann and Heinzle (26).

^{13}C-labeling analysis. Mass isotopomer fractions of lysine and trehalose were required for calculation of metabolic flux. They were quantified by GC-MS from lyophilized cultivation supernatants (10). Mass isotopomer fractions are defined as M_0 (relative amount of unlabeled mass isotopomer), M_1 (relative amount of single-labeled mass isotopomers), and corresponding terms for higher labeling. Analysis of lysine was performed after derivatization into the *t*-butyl-dimethylsilyl derivative (27). The ion cluster at a mass-to-charge ratio (*m*/*z*) of 431 to 437, representing a fragment with the complete carbon skeleton of lysine, was measured in selective ion monitoring (SIM) mode. The labeling pattern of trehalose was determined in SIM mode from its trimethylsilyl derivative via the ion cluster at *m*/*z* 361 to 367, corresponding to a fragment ion that contains an entire monomer unit of trehalose and thus a carbon skeleton equal to that of glucose-6-phosphate (28). All samples were measured first in scan mode to exclude isobaric interference between analyzed products and other sample components. All measurements in SIM mode were performed in duplicate. The mean experimental error for the mass isotopomer fractions was 0.17%.

For manual inspection of the metabolic network, the measured mass isotopomer fractions of lysine and the trehalose monomer were corrected for natural isotopes (21). The outputs of the correction were mass isotopomer fractions of the carbon skeleton of the analytes ($M_{i,\mathrm{corr}}$). The total ^{13}C enrichment of the carbon skeleton of a compound with *n* carbon atoms, termed summed fractional labeling (SFL) (6), was calculated according to equation 1:

$$\mathrm{SFL} = \sum_{i=1}^{n+1} \frac{i \cdot M_{i,\mathrm{corr}}}{\mathrm{n}} \quad (1)$$

Metabolic modeling and parameter estimation. All metabolic simulations were carried out on a personal computer using Matlab 6.5 and Simulink 3.0 (Mathworks Inc., Nattick, Mass.). Details on the computational tools used are given elsewhere (26). The metabolic network for growth and lysine production of *C. glutamicum* on sucrose comprised all central metabolic pathways, i.e., glycolysis, the pentose phosphate pathway (PPP), the tricarboxylic acid (TCA) cycle, and anaplerotic carboxylation. Additionally, the pathways for the biosynthesis of lysine and different by-products (Table 1) and the anabolic pathways from intermediary precursors into biomass (Table 2) were included. For uptake of sucrose, the corresponding PTS with phosphorylation into sucrose-6-phosphate and subsequent hydrolysis into glucose-6-phosphate and fructose was included in the network (14). For fructose utilization, PTS^{Fru}, 1-phosphofructokinase, and PTS^{Man} were included (3). Fructose-1,6-bisphosphatase was assumed to be inactive due to lack of activity during growth of *C. glutamicum* on glucose and fructose (4). Reactions regarded as catalyzed by reversible were those transaldolase and transketolases in the PPP and glucose-6-phosphate isomerase. The reversibilities of these reactions were quantified during the flux estimation procedure. Anaplerotic carboxylation from the lumped pools of phosphoenolpyruvate-pyruvate to malate-oxaloacetate and the TCA cycle reactions between malate dehydrogenase and fumarate hydratase were regarded as irreversible (10) Based on previous results, the glyoxylate pathway was assumed to be inactive (26).

Calculation of the anabolic demand for the different precursors was based on refined data on the biomass composition of *C. glutamicum* (24), which considered the specific anabolic demand for cell wall synthesis based on the diaminopimelate content of the cell. The anabolic demands of the different precursors were corrected for the actual auxotrophic demand of the examined strain for threonine, methionine, and leucine. Overall, an NADPH demand of 12 mM (g [dry mass] of cell)$^{-1}$ resulted for the examined strain *C. glutamicum* ATCC 21526. The data on biomass composition used in the present work differed slightly from those of a previous study with the same strain on glucose and fructose (10). To exclude a possible influence of the different biomass compositions, fluxes for glucose and fructose were recalculated with the actual data on cellular composition. The results obtained did not differ significantly from previous data. As an example, fluxes through the PPP by previous and present estimations were almost identical (15 and 16% for fructose-grown cells; 62 and 63% for glucose-grown cells). Due to this, the different anabolic demands do not interfere with quantitative comparisons between the two studies. Labeling data of secreted lysine and trehalose and means of the stoichiometric data from the three independent tracer experiments with different sucrose labelings were combined for calculation of metabolic flux. The set of fluxes that gave minimum deviation between experimental ($M_{i,\mathrm{exp}}$) and simulated ($M_{i,\mathrm{calc}}$) mass isotopomer fractions was taken as the best estimate for intracellular flux distribution. The network of sucrose-grown cells was overdetermined, so that a least-squares approach was possible. As an error criterion, a weighted sum of least squares (SLS) was used, where $S_{\mathrm{i,exp}}$ is the standard deviation of the measurements (equation 2):

$$\mathrm{SLS} = \sum_i \frac{(M_{i,\mathrm{exp}} - M_{i,\mathrm{calc}})^2}{S_{i,\mathrm{exp}}{}^2} \quad (2)$$

Identical flux distributions were obtained with multiple randomized initialization values, suggesting that a global minimum was identified. Statistical analysis of the fluxes obtained was carried out by a Monte Carlo approach (26). From the data obtained, 90% confidence limits for the single parameters were calculated. In additional flux calculations, the assumed network topology was varied to investigate the consequences of a lack of the two fructose transporters (PTS^{Fru},

TABLE 2. Anabolic demand of *C. glutamicum* ATCC 21526 for intracellular metabolites in the process of lysine production from sucrose

Anabolic precursor	Demand [mmol (mol sucrose)$^{-1}$][a]
Glucose-6-phosphate	11.05 ± 0.08
Fructose-6-phosphate	16.61 ± 0.12
Pentose-5-phosphate	47.41 ± 0.35
Erythrose-4-phosphate	14.45 ± 0.11
Glyceraldehyde-3-phosphate	6.96 ± 0.05
3-Phosphoglycerate	69.86 ± 0.52
Pyruvate-phosphoenolpyruvate	117.27 ± 0.87
α-Ketoglutarate	66.02 ± 0.49
Oxaloacetate	46.12 ± 0.34
Acetyl coenzymeA	147.65 ± 1.09
Diaminopimelate + lysine[b]	18.76 ± 0.14

[a] Values are means (and standard deviations) from parallel incubations on 20 mM [1-$^{13}C^{Fru}$]sucrose, 20 mM [1-$^{13}C^{Glc}$]sucrose, and 20 mM[$^{13}C_6{}^{Fru}$]sucrose. The calculation of the anabolic demand is based on the experimental biomass yield (Table 1) and on the cellular composition of *C. glutamicum* (24).

[b] Diaminopimelate and lysine are regarded as separate anabolic precursors. This is due to the fact that anabolic fluxes from pyruvate and oxaloacetate into diaminopimelate (cell wall) and lysine (protein) contribute, in addition to the flux of lysine secretion, to the overall flux through the lysine biosynthetic pathway.

PTS^{Man}) and the presence of an active fructose-1,6-bisphosphatase on the fluxes obtained and the goodness of fit.

RESULTS AND DISCUSSION

Cultivation of lysine-producing *C. glutamicum* on sucrose. (i) Growth and lysine production. *C. glutamicum* ATCC 21526 produced 11 mM lysine and 1.1 g [dry mass] of cells $liter^{-1}$ from 20 mM consumed sucrose. This corresponds to a lysine yield ($Y_{Lys/S}$) of 137 mmol mol^{-1} and a biomass yield ($Y_{X/S}$) of 13.5 mg $mmol^{-1}$. Comparison of the yields obtained from sucrose with those from other carbon sources provides an interesting picture. For a direct comparison with data from hexose sugars, the yields given above, which are expressed per mole of sucrose, i.e., per 2 mol of hexose, are multiplied by a factor of 2. This leads to a $Y_{Lys/S}$ of 274 mmol (mol of hexose)$^{-1}$ and a $Y_{X/S}$ of 27 mg (mmol of hexose)$^{-1}$. A similar $Y_{Lys/S}$ [281 mmol (mol of hexose)$^{-1}$] was previously achieved with the same strain by using glucose as the carbon source (10). The two substrates differed markedly, however, with respect to the biomass formed. The biomass yield on sucrose was only 50% of that found for glucose. Cultivation on sucrose thus involves a significantly lower demand for anabolic precursors and cofactors.

Lysine production on sucrose was much better than that on fructose [$Y_{Lys/S}$ = 244 mmol (mol of hexose)$^{-1}$], whereas the two substrates resulted in similar biomass yields. *C. glutamicum*, cultured on sucrose, maintained the high production capability found for glucose, despite the fact that the disaccharide sucrose contains 50% of the low-yield monomer fructose. Lysine production by *C. glutamicum* on sucrose was therefore not a simple superposition of the situations with glucose and fructose. During incubation, the cell concentration increased from 3.5 to 4.6 g $liter^{-1}$. Due to the fact that essential amino acids were not present in the medium, internal sources were probably utilized by the cells for biomass synthesis. Overall, use of sucrose as a carbon source resulted in completely different fluxes toward anabolic pathways and lysine biosynthesis than use of glucose or fructose. Lysine production by another strain, *C. glutamicum* ATCC 21253, previously showed similar effects of sucrose, glucose, and fructose on growth and product formation (9), indicating that the behavior observed might be typical for lysine-producing corynebacteria.

(ii) Substrate uptake. During growth of *C. glutamicum* on sucrose, a low fructose concentration of about 50 μM was observed in the medium and no extracellular glucose was detected. This shows that fructose undergoes transient secretion. The reassimilation of fructose is catalyzed by fructose uptake systems. Mutants of *C. glutamicum* lacking functioning uptake systems for fructose show extracellular fructose accumulation during metabolization of sucrose (3). The low concentration of fructose points to a high affinity of these uptake systems. For the subsequent flux calculation, complete consumption of fructose and glucose could be assumed. The amount of extracellular fructose was only about 0.1% of total carbon consumed and thus was negligible. The mean specific uptake rate for sucrose was 0.8 mmol g^{-1} h^{-1}. The corresponding uptake flux for single hexose units was 1.6 mmol g^{-1} h^{-1}. These rates were comparable to those for glucose-grown cells. Thus, similar carbon fluxes enter the cells on these two industrially important carbon sources (10). The sucrose uptake rate was about 20% lower than that of fructose.

(iii) By-product formation. Different by-products such as trehalose, amino acids, organic acids, and alcohols were formed during the cultivation (Table 1). The main by-product was dihydroxyacetone. Note that dihydroxyacetone is not reutilized by *C. glutamicum* and therefore displays wasted carbon with respect to lysine biosynthesis (4). This compound, together with glycerol, stems from dihydroxyacetone phosphate. Secretion of these products by *C. glutamicum* was found to depend on the carbon source used (10). Significant formation of glycerol and dihydroxyacetone was observed for growth on fructose, whereas only minor secretion was observed for growth on glucose. It is assumed that the high glycolytic flux on fructose exceeds the capacity of glycolytic enzymes such as glyceraldehyde-3-phosphate, leading to the observed overflow metabolism (4). It seems that, to a lesser extent, the metabolic capacity of the glycolytic chain is also exceeded when sucrose is used as the carbon source. The fact that this was less pronounced could be due to the composition of sucrose, which contains only 50% of the overflow favoring fructose. The phenomenon of a differing degree of overflow metabolism depending on the glycolytic flux is well known for other organisms such as *Saccharomyces cerevisiae* (5). The sum of the yield coefficients of dihydroxyacetone and glycerol was close to the corresponding mean for glucose and fructose (10). Thus, with regard to the formation of these specific by-products, the behavior of sucrose was equivalent to the average of the behaviors of its two monomers.

Interestingly, this was not the case for the yield coefficient of trehalose, which was twofold higher than that for *C. glutamicum* cells grown under comparable conditions on glucose and about fivefold higher than that for fructose-grown cells (10). A low trehalose yield was previously related to a low availability of glucose-6-phosphate, the precursor for trehalose phosphate formation (15). This could indicate an increased intracellular glucose-6-phosphate level when sucrose is used as the carbon source, probably the consequence of the different entry points of glucose and fructose into the central metabolism. Trehalose secretion by *C. glutamicum* could be blocked by disruption of the corresponding trehalose biosynthetic pathways (19, 29).

As indicated by the low deviation for the yield coefficients obtained, good agreement between parallel experiments was achieved (Table 1). It therefore seemed justified to combine all experimental data for metabolic flux calculation.

Pathway identification in lysine-producing *C. glutamicum* on sucrose. In each of the experiments, the two monomer units of sucrose, glucose and fructose, had different ^{13}C enrichment. ^{13}C enrichment of lysine and trehalose, determined by SFL, therefore provides direct information on the extent to which each of the two monomers was utilized for their synthesis. Based on this, some important basic characteristics of the metabolism of *C. glutamicum* on sucrose can be investigated. One hundred percent labeling enrichment was assumed for the tracer substrates, and reversible reactions were neglected. The principle of this approach can be illustrated for the study with [$^{13}C_6^{Fru}$]sucrose. The completely labeled fructose monomer of this substrate has an SFL of 1, and the SFL of the unlabeled glucose monomer is 0. A product formed exclusively from the fructose monomer is then completely labeled, i.e., exhibits an

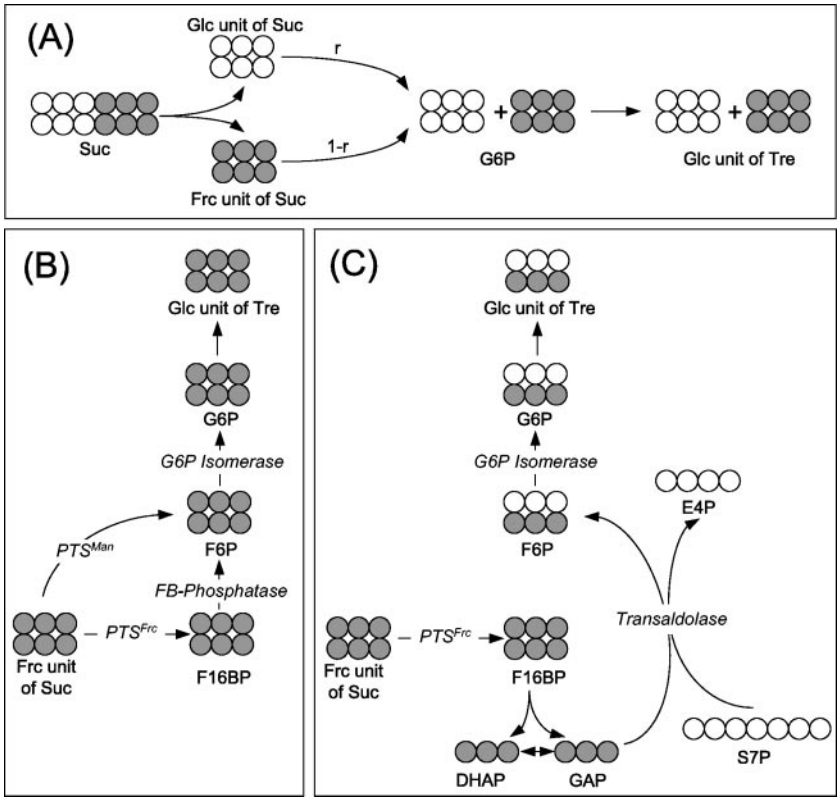

FIG. 1. Transition of carbon from the tracer substrate [$^{13}C_6{}^{Fru}$]sucrose to glucose-6-phosphate (G6P) as a precursor of the trehalose monomer. (A) Relationship between the labeling of the trehalose monomer and the relative contributions of the two sucrose residues, glucose (r) and fructose ($1 - r$), to its synthesis. (B) Formation of the fully ^{13}C labeled trehalose monomer from an entire fructose residue of sucrose by PTS^{Man} and glucose-6-phosphate. The alternative route shown via PTS^{Fru} and fructose-1,6-bisphosphatase cannot be completely excluded, due to identical isotopic labeling, but appears unlikely due to previous enzymatic measurements for *C. glutamicum* (4). (C) Formation of the triple ^{13}C labeled trehalose monomer from the fructose residue of sucrose by concerted action of fructose-1,6-bisphosphate aldolase, transaldolase, and glucose-6-phosphate isomerase. DHAP, dihydroxyacetone phosphate; GAP, glyceraldehyde-3-phosphate; F6P, fructose-6-phosphate; S7P, sedoheptulose-7-phosphate; E4P, erythrose-4-phosphate; F16BP, fructose-1,6-bisphosphate; Suc, sucrose; Glc, glucose.

SFL of 1. A product originating from the glucose monomer is unlabeled (SFL = 0). Contribution of both substrate parts leads to a value between 0 and 1.

(i) Relative contribution of central pathways to trehalose formation. The transition of the ^{13}C label from the tracer substrate [$^{13}C_6{}^{Fru}$]sucrose to the monomer unit of trehalose is diagrammed in Fig. 1A. Obviously, the relative fractions of the $^{13}C_6$ and the $^{12}C_6$ mass isotopomer of the product are directly proportional to the relative contributions of the two substrate residues, glucose (r) and fructose ($1 - r$). A simple relation between the SFL of the trehalose monomer, experimentally obtained by GC-MS analysis of its trimethylsilyl derivative at m/z 361 to 367, and the relative supply from the fructose residue ($1 - r$) can be formulated (equation 3). Here, an SFL of 0.5 for the substrate [$^{13}C_6{}^{Fru}$]sucrose is considered.

$$SFL_{\text{trehalose monomer}} = 2 \cdot (1 - r) \cdot SFL_{[^{13}C_6{}^{Fru}]\text{sucrose}} = (1 - r) \quad (3)$$

According to equation 3, the theoretical SFL of the trehalose monomer varies between 1 for sole formation from the fructose residue ($r = 0$) and 0 for sole formation from the glucose residue ($r = 1$) (Table 3). The experimental SFL for the trehalose monomer was 0.24, resulting in an r of 0.76, i.e., 76% of the trehalose monomer originated from the glucose residue of the substrate. This clearly shows that glucose is the main pre-

TABLE 3. SFL of sucrose and trehalose in cultivations of lysine-producing *C. glutamicum* on [1-$^{13}C^{Fru}$]sucrose, [1-$^{13}C^{Glc}$]sucrose, and [$^{13}C_6{}^{Fru}$]sucrose[a]

Tracer substrate	SFL of:			r
	Sucrose	Trehalose monomer		
		Calc.	Exp.	
[$^{13}C_6{}^{Fru}$]sucrose	0.50	0.00 ($r = 1$) 0.50 ($r = 0.5$) 1.00 ($r = 0$)	0.24	0.76
[1-$^{13}C^{Fru}$]sucrose	0.08	0.00 ($r = 1$) 0.08 ($r = 0.5$) 0.17 ($r = 0$)	0.05	0.71
[1-$^{13}C^{Glc}$]sucrose	0.08	0.17 ($r = 1$) 0.08 ($r = 0.5$) 0.00 ($r = 0$)	0.12	0.71

[a] The SFL is given for the entire substrate molecule and the trehalose monomer; the latter equals that of glucose-6-phosphate. The theoretical (Calc.) SFL of the trehalose monomer is calculated by assuming sole formation from glucose ($r = 1$) or from fructose ($n = 0$), or equal formation from both residues ($n = 0.5$), according to equation 3. The experimental (Exp.) SFL of the trehalose monomer was obtained by GC-MS analysis of the trimethylsilyl derivative of trehalose at an m/z of 361 to 367 with subsequent correction for natural isotopes. The data are used to determine the relative contribution of glucose to the formation of the trehalose monomer (r).

cursor for the synthesis of trehalose. The labeling of the measured trehalose fragment directly represents that of glucose-6-phosphate, which is the entry metabolite into the oxidative part of the PPP. The relative contributions of fructose and glucose to formation of the trehalose monomer are therefore identical to their relative entrance into this pathway. One can therefore conclude that the major fraction of carbon entering the PPP during *C. glutamicum* growth on sucrose originates from the glucose part of the substrate.

The approach used for [$^{13}C_6^{Fru}$]sucrose also allows the determination of *r*, by similar equations, for the other tracer substrates used. Applying the same principle here yields almost identical values for the relative contributions of glucose and fructose to trehalose synthesis (Table 3). The high supply of glucose-6-phosphate by the glucose residue is also reflected by the mass isotopomer distribution of the trehalose unit (Fig. 2A). Fractions of higher labeling were significantly enriched when [1-$^{13}C^{Glc}$]sucrose was used, whereas they were only slightly enriched when [1-$^{13}C^{Fru}$]sucrose was used.

The formation of glucose-6-phosphate from the glucose residue of sucrose is directly linked to the cleavage of sucrose-6-phosphate formed during the uptake of sucrose into cells. The situation for the fructose part is, however, more complex. A closer inspection of the underlying metabolic routes can be obtained from the mass isotopomer distribution of the measured trehalose fragment for [$^{13}C_6^{Fru}$]sucrose as a substrate (Fig. 2A). Here, significant fractions of triple-labeled (M_3) and fully labeled mass isotopomers were observed. The fully labeled trehalose monomer reflects the fully labeled mass isotopomer of its precursor, glucose-6-phosphate. A possible metabolic route for production of fully ^{13}C labeled (M_6) glucose-6-phosphate is provided by the concerted action of PTS^{Man} and reversible glucose-6-phosphate isomerase, which convert entire C_6 units from the fructose part of the substrate into glucose-6-phosphate (Fig. 1B). The occurrence of M_3 mass isotopomers points to additional reactions that are involved in the supply of glucose-6-phosphate. These comprise the action of fructose-1,6-bisphosphate aldolase, which cleaves fully labeled fructose-1,6-bisphosphate originating from the fructose residue of [$^{13}C_6^{Fru}$]sucrose into fully labeled C_3 units (Fig. 1C). By the reversible action of transaldolase in the PPP, these labeled C_3 units are combined with unlabeled carbons from sedoheptulose-7-phosphate, which then leads to the formation of M_3 mass isotopomers of fructose-6-phosphate and glucose-6-phosphate. Note that all carbons of glyceraldehyde-3-phosphate are transferred to fructose-6-phosphate by the action of transaldolase (16). The relative occurrences of M_3 and M_6 mass isotopomers of the measured trehalose fragment for [$^{13}C_6^{Fru}$]sucrose can be used to assess the relative activities of these two alternative routes (Fig. 2A). It is assumed that the M_3/M_6 ratio of the trehalose monomer is directly proportional to the relative contributions of the two metabolic routes (Fig. 1B and C). Based on this assumption, 20% of the trehalose originates from uptake via PTS^{Man}. A relative fraction of about 80% is supplied by recycling of carbon from the level of glyceraldehyde-3-phosphate through the reversible PPP reactions. These reactions therefore comprise the major pathway for the redirection of carbon from the fructose unit to glucose-6-phosphate and thus into the NADPH-generating oxidative part of the PPP. On fructose also, they exhibit significant in vivo activity and contribute to the supply of glucose-6-phosphate and subsequently to the formation of NADPH (10).

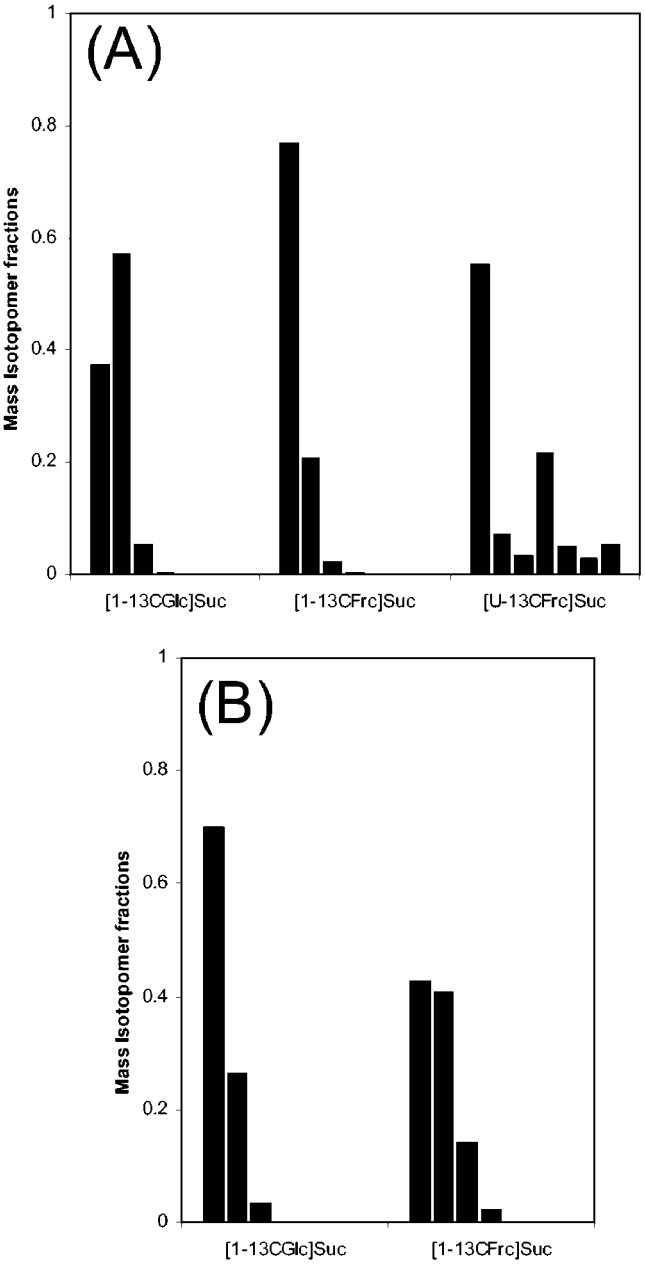

FIG. 2. Mass isotopomer distributions of the carbon skeletons of glucose-6-phosphate (A) and lysine (B) during cultivation of *C. glutamicum* ATCC 21526 on [1-$^{13}C^{Fru}$]sucrose, [1-$^{13}C^{Glc}$]sucrose, and [$^{13}C_6^{Fru}$]sucrose, respectively. The data were calculated from GC-MS measurements of the *m/z* 361 ion cluster of trimethylsilyl-derivatized trehalose, corresponding to the carbon skeleton of glucose-6-phosphate, and of the *m/z* 431 ion cluster of *t*-butyl-trimethylsilyl-derivatized lysine by correcting for natural isotopes as described by van Winden et al. (21).

Uptake through the PTS^{Fru} and subsequent conversion through gluconeogenesis theoretically constitutes a further alternative for producing fully labeled glucose-6-phosphate from [$^{13}C_6^{Fru}$]sucrose (Fig. 1B). However, this would require an active fructose bisphosphatase. Previously this enzyme was not

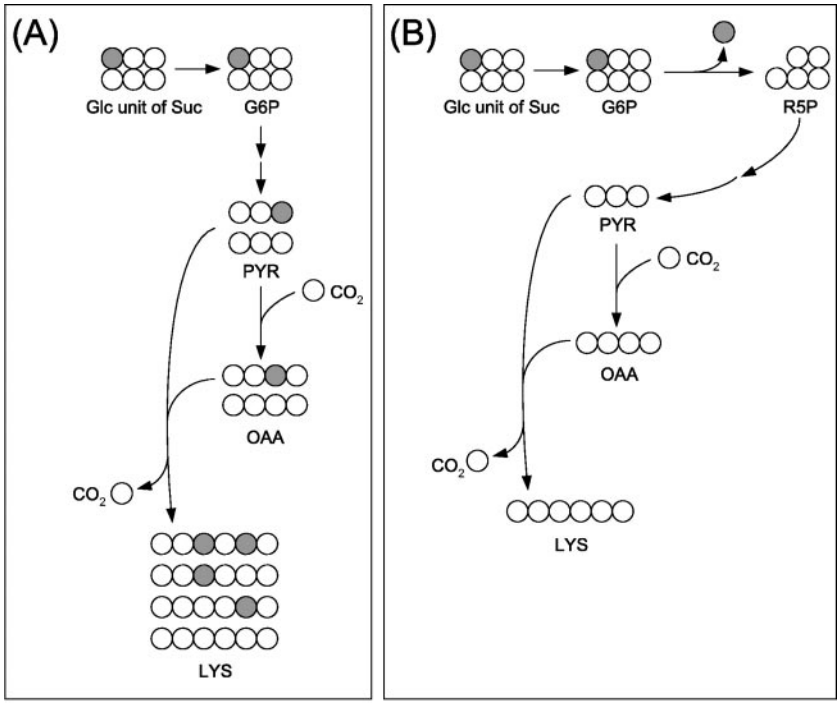

FIG. 3. Transition of carbon from the glucose residue of [1-$^{13}C^{Glc}$]sucrose to lysine. Shown is metabolization of the glucose unit via glycolysis with complete ^{13}C label conservation (A) and via the PPP with complete ^{13}C label release as CO_2 (B). PYR, pyruvate; OAA, oxaloacetate; R5P, ribose-5-phosphate; Lys, lysine.

found to be active in *C. glutamicum* cultured on glucose or fructose (4).

(ii) Relative contribution of central pathways to lysine formation. Interpretation of the labeling data of lysine provides further insights into the metabolic network of *C. glutamicum* during lysine production on sucrose. The ^{13}C labeling pattern of lysine differed strongly between [1-$^{13}C^{Glc}$]sucrose and [1-$^{13}C^{Fru}$]sucrose (Fig. 2B). This provides the first evidence that the two monomers of the substrate do not contribute equally to the formation of lysine. A deeper insight into the underlying metabolic reactions can be gained by consideration of the metabolic fate of the glucose monomer of [1-$^{13}C^{Glc}$]sucrose (Fig. 3). If the [1-^{13}C] glucose monomer is completely channeled through glycolysis, the ^{13}C labeling is completely conserved in the carbon skeleton of pyruvate (Fig. 3A). As a result, significant fractions of double-labeled and single-labeled lysine are formed. However, the lysine pool is completely unlabeled (SFL = 0) when the glucose monomer is converted exclusively via the PPP, due to complete release of the labeled carbon as CO_2 (Fig. 3B). The additional use of the unlabeled fructose unit for lysine formation dilutes the labeling of the lysine pool, so that the SFL of lysine is proportional to the relative flux (q) of the glucose monomer into the PPP (equation 4).

$$SFL_{lysine} = SFL_{[1\text{-}^{13}C^{Glc}]sucrose} \cdot q = 0.08 \cdot q \qquad (4)$$

The experimental SFL determined for lysine during growth of *C. glutamicum* on [1-$^{13}C^{Glc}$]sucrose was 0.04, significantly below that of the substrate (Table 4). This gives a fraction of about 50% of the glucose part of sucrose that is directed into the PPP. It should be noted that this value for q displays only the minimal fraction of glucose directed into the PPP. Due to the reversible action of glucose-6-phosphate isomerase (26), a significant amount of the glucose-6-phosphate pool is probably unlabeled, originating from unlabeled fructose-6-phosphate out of the PPP. This leads to an underestimation of q, so that the value obtained is equal to a lower boundary for the PPP flux from the glucose monomer.

Manual inspection of the labeling data provides some interesting insights into the metabolic network of *C. glutamicum* during lysine production on sucrose. Almost identical results were obtained from three independent experiments for the contributions of the glucose and fructose residues to the supply of glucose-6-phosphate. This underlines the high consistency of the studies performed. The manual interpretation of the data, however, is based on certain simplifications such as ignoring reversible reactions. Additionally, a number of important flux parameters cannot be assessed. Therefore, this ap-

TABLE 4. SFL of sucrose and lysine, from cultivation of lysine-producing *C. glutamicum* on [1-$^{13}C^{Glc}$]sucrose[a]

Tracer substrate	SFL of:			q
	Sucrose	Lysine		
		Calc.	Exp.	
[1-$^{13}C^{Glc}$]sucrose	0.08	0.00 (q = 1) 0.08 (q = 0)	0.04	0.50

[a] The theoretical (Calc.) SFL of lysine is calculated by assuming sole formation from glucose (r = 1) or from fructose (r = 0). The experimental (Exp.) value was obtained by GC-MS analysis of the *t*-butyl-dimethylsilyl derivative of lysine at an m/z of 431 to 437 with subsequent correction for natural isotopes. The data are used to determine the relative flux of the glucose monomer of the substrate sucrose into the PPP (q) according to equation 4.

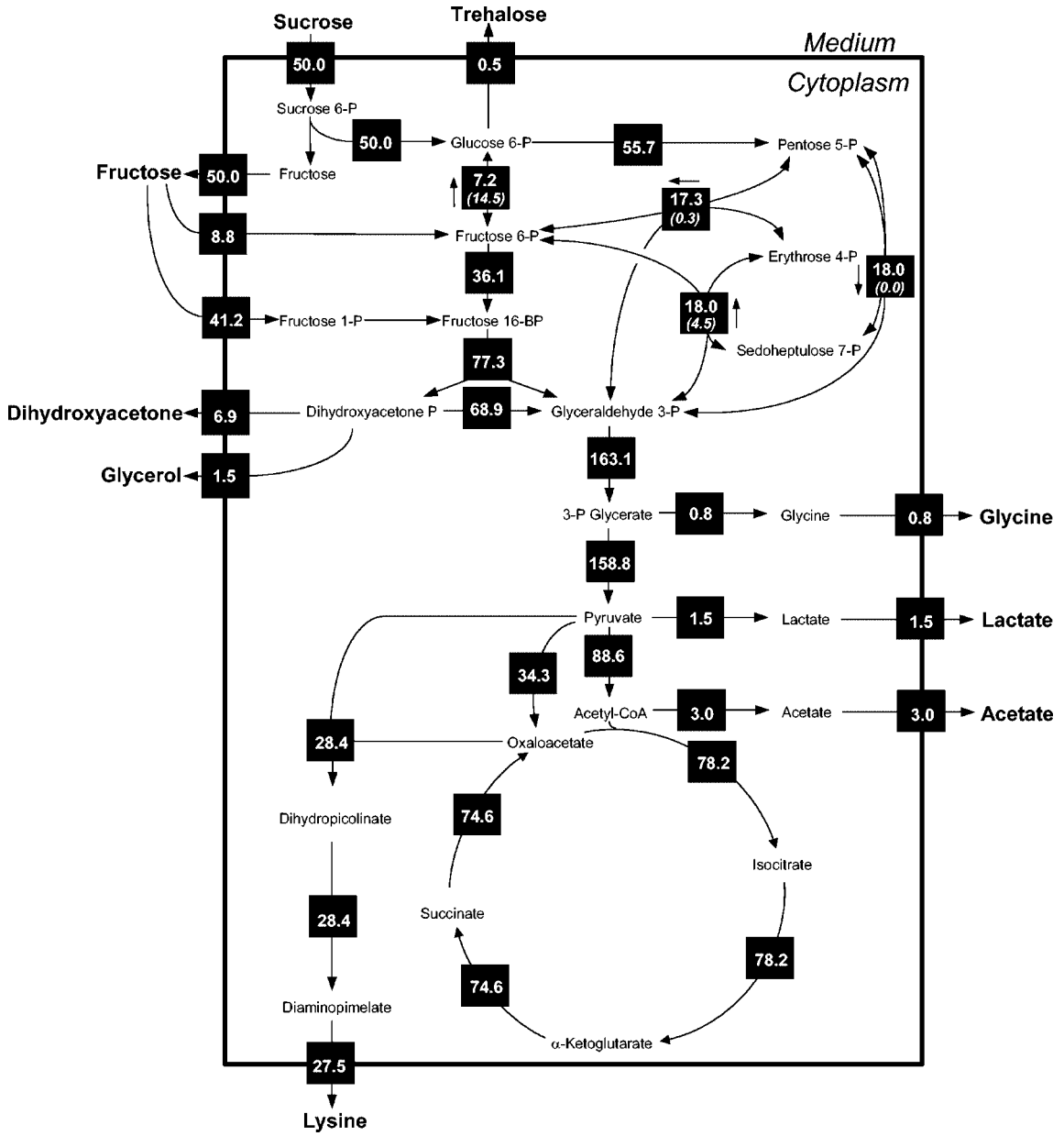

FIG. 4. In vivo carbon flux distribution in the central metabolism of *C. glutamicum* ATCC 21526 during lysine production on sucrose. The fluxes were estimated from the best fit to the experimental results by using a comprehensive approach of combined metabolite balancing and isotopomer modeling for three independent ^{13}C tracer experiments on [1-$^{13}C^{Fru}$]sucrose, [1-$^{13}C^{Glc}$]sucrose, and [$^{13}C_6{}^{Fru}$]sucrose, respectively, and labeling measurement of secreted lysine and trehalose by GC-MS. Net fluxes are given in solid squares; for reversible reactions, the direction of the net flux is indicated by an arrow along one side of the solid square. Numbers in parentheses given below the fluxes of reversible reactions indicate flux reversibilities. All fluxes are expressed as molar percentages of the mean specific sucrose uptake rate (0.8 mmol g^{-1} h^{-1}), which is set to 50% so as to facilitate comparison with other flux maps, which are usually derived from hexose substrates.

proach is limited. As an example, it provides only a lower boundary for the relative flux of glucose into the PPP instead of a real flux value. These limitations can be overcome by a ^{13}C flux model that involves metabolite and isotopomer balancing for the calculation of metabolic fluxes (26). Here, a comprehensive data set of ^{13}C labeling data and stoichiometric data is used to obtain the fluxes. Such a model, which fully considers, e.g., label transition by bidirectional reactions, label scrambling in symmetric molecules, and ^{13}C incorporation from CO_2 or naturally occurring isotopes in the tracer substrate, was used to quantitatively determine the actual fluxes of *C. glutamicum* during lysine production on sucrose.

Intracellular fluxes of lysine-producing *C. glutamicum* on sucrose. The obtained metabolic flux distribution of lysine-producing *C. glutamicum* on sucrose is shown in Fig. 4. With regard to the fit obtained, excellent agreement between experimentally determined and calculated mass isotopomer ratios was achieved (Table 5). Statistical analysis revealed a generally high precision for the fluxes obtained, as indicated by the narrow 90% confidence intervals (Table 6).

TABLE 5. Relative mass isotopomer fractions of lysine and trehalose secreted during cultivation of lysine-producing *C. glutamicum* ATCC 21526 on [1-$^{13}C^{Fru}$]sucrose, [1-$^{13}C^{Glc}$]sucrose, and [$^{13}C_6{}^{Fru}$]sucrose[a]

Product	[1-$^{13}C^{Fru}$]sucrose				[1-$^{13}C^{Glc}$]sucrose				[1-$^{13}C_6{}^{Fru}$]sucrose			
	M_0	M_1	M_2	M_3	M_0	M_1	M_2	M_3	M_0	M_1	M_2	M_3
Lysine												
Exp.	0.283	0.362	0.223	0.093	0.464	0.323	0.147	0.050	0.050	0.082	0.143	0.193
Calc.	0.283	0.361	0.222	0.094	0.466	0.319	0.148	0.050	0.049	0.079	0.151	0.195
Trehalose												
Exp.	0.540	0.283	0.126	0.037	0.261	0.473	0.173	0.071	0.396	0.151	0.090	0.177
Calc.	0.536	0.290	0.126	0.038	0.252	0.484	0.173	0.072	0.420	0.156	0.088	0.170

[a] Data are given as experimental (Exp.) GC-MS data of the *m/z* 431 ion cluster of *t*-butyl-trimethylsilyl-derivatized lysine or of the *m/z* 361 ion cluster of trimethysilyl-derivatized trehalose and as values predicted by the solution of the mathematical model corresponding to the optimized set of fluxes (Calc.). M_0, relative amount of unlabeled mass isotopomer fraction; M_1, relative amount of the single-labeled mass isotopomer fraction; corresponding terms stand for higher labeling.

(i) Substrate uptake. Sucrose entered the cells with a flux of 50%, equal to the observed mean specific uptake rate of 0.8 mmol of sucrose g^{-1} h^{-1}. It was subsequently converted into equimolar amounts of glucose-6-phosphate and fructose. Fructose exhibited transient secretion into the medium and was completely reassimilated. Both PTSs contributed in vivo to the uptake of fructose. The predominant fraction of fructose was reassimilated through PTS^{Fru}, whereas only a low flux of 8.8% resulted for PTS^{Man}. Thus, the majority of fructose entered glycolysis at the level of fructose-1,6-bisphosphate, while only a small fraction was channeled upstream at fructose-6-phosphate into the glycolytic chain.

Omitting either PTS^{Man} or PTS^{Fru} as an uptake system for fructose from the metabolic network model resulted in significantly worse agreement between experimental and simulated labeling data (data not shown). In both cases the sum of residuals increased more than 15-fold. The deviation between measured and simulated labeling data for trehalose from the tracer study with [$^{13}C_6{}^{Fru}$]sucrose increased up to >50% when one of the transporters was removed from the model. Therefore, a simplified model with only a single PTS for fructose uptake obviously could not describe the experimental data. Activity of both fructose transporters was necessary in order to obtain a reasonable fit. This underlines the fact that both transporters are contributing in vivo to the uptake of fructose.

(ii) Metabolic flux through glycolysis and PPP. The relative flux into the PPP was 55.7%. Thus, a significant amount of carbon was directed toward the PPP for NADPH formation. The PPP flux could be determined with high precision, as shown by the narrow 90% confidence interval of only about 3% (Table 6). The labeling data thus very sensitively reflected this important flux parameter. The PPP flux was even higher then the 50% uptake flux of the glucose monomer. This indicates that the carbon entering the PPP originated from other reactions as well. In fact, glucose-6-phosphate isomerase operated in the gluconeogenetic direction, i.e., from fructose-6-phosphate to glucose-6-phosphate. By the action of this enzyme, an additional 7.2% of carbon was channeled from fructose-6-phosphate toward the PPP. Due to the activity of PTS^{Man} (8.8%), transketolase 2 (17.3%), and transaldolase (18.0%), a total flux of 44.1% arrived at the pool of fructose-6-phosphate and was potentially available to be channeled through the PPP. However, most of the carbon entering the pool of fructose-6-phosphate was drained off into the lower glycolysis by the significant activity (36.8%) of 6-phosphofructokinase.

The enormous metabolic flexibility of *C. glutamicum* may be visualized by comparing the fluxes obtained on sucrose with previous flux data on glucose and fructose (10). An interesting picture is yielded by relating the flux into the PPP to the total flux toward glucose-6-phosphate, i.e., the maximum flux available for direction into the PPP under the given conditions. On sucrose, this fraction was 97%. The carbon from the glucose-6-phosphate pool was thus almost exclusively directed into the PPP. On glucose, this fraction is only about 50 to 70% (10). The resulting PPP flux for sucrose-grown *C. glutamicum* cells was about 40% higher than that for fructose-grown cells. The difference was thus slightly less than the additional uptake flux

TABLE 6. Statistical evaluation of metabolic fluxes of lysine-producing *C. glutamicum* ATCC 21526 during growth on sucrose

Flux parameter	90% Confidence interval[a]
Net flux	
Fructose uptake by PTS^{Fru}	80.3–84.6
Fructose uptake by PTS^{Man}	15.4–19.7
Glucose-6-phosphate isomerase	6.0–8.9
1-phosphofructokinase	80.3–84.6
6-phosphofructokinase	34.6–37.3
Fructose-1, 6-bisphosphate aldolase	76.6–77.8
Glucose-6-phosphate dehydrogenase	54.3–57.6
Transaldolase	17.6–18.6
Transketolase 1	17.6–18.6
Transketolase 2	16.8–17.9
Glyceraldehyde-3-phosphate dehydrogenase	161.1–165.5
Pyruvate kinase	156.7–160.1
Pyruvate dehydrogenase	83.0–93.6
Pyruvate carboxylase	31.8–36.9
Citrate synthase	71.6–83.6
Isocitrate dehydrogenase	71.6–83.6
Oxoglutarate dehydrogenase	68.0–80.0
Aspartokinase	25.9–31.0
NADPH supply by PPP and isocitrate dehydrogenase	180.9–198.7
NADPH demand for lysine production and growth	134.7–156.5
Flux reversibility[b]	
Glucose-6-phosphate isomerase	11.3–21.6
Transaldolase	3.8–5.2
Transketolase 1	0.0–0.0
Transketolase 2	0.0–0.6

[a] The 90% confidence intervals of the flux parameters were obtained by a Monte Carlo approach including 100 independent parameter estimation runs with stastically varied experimental data.

[b] Flux reversibility is defined as the ratio of back flux to net flux.

of the glucose monomer of sucrose. In both cases, however, the PPP flux is clearly determined by the carbon flux through glucose-6-phosphate isomerase. However, amplification of this enzyme would not necessarily lead to significant changes in the net fluxes, due to its highly reversible nature. Obviously, glucose-6-phosphate isomerase is an important enzyme for metabolic flexibility of *C. glutamicum*. The highly reversible nature of this enzyme, observed in vivo in previous studies (25, 26), plays an important role in adaptation of intracellular fluxes to environmental conditions, i.e., a change of carbon source. As shown, glucose-6-phosphate isomerase works in the glycolytic direction, i.e., from glucose-6-phosphate to fructose-6-phosphate, during growth on sucrose and glucose, whereas the opposite flux direction is found for fructose-grown cells (10). The thermodynamic equilibrium constant of glucose-6-phosphate isomerase is about 0.3 (30). Accordingly, for a net flux in the glycolytic direction (from glucose-6-phosphate to fructose-6-phosphate), the concentration of glucose-6-phosphate must be at least threefold higher than that of fructose-6-phosphate. Previous intracellular measurements in *C. glutamicum* showed a glucose-6-phosphate/fructose-6-phosphate ratio of 2.7 for growth on glucose, indicating that the enzyme is operating close to equilibrium under these conditions (4). To achieve a net flux in the opposite direction (from fructose-6-phosphate to glucose-6-phosphate), the concentration ratio must be lower than 3. During growth on fructose, however, a ratio of 7.5 was observed (4). This seems to contradict the actual flux data and is probably related to errors in the intracellular metabolite measurements.

Only a small fraction (7.2%) of the total flux of 44.1% arriving at the pool of fructose-6-phosphate was utilized by the strain for gluconeogenetic formation of glucose-6-phosphate by glucose-6-phosphate isomerase. Thus, only 16% of the total carbon entering the pool of fructose-6-phosphate was converted through glucose-6-phosphate isomerase toward the oxidative part of the PPP. A rather different behavior is found for fructose-grown *C. glutamicum* cells, which exhibit a gluconeogenetic flux through 6-phosphate isomerase of 15.2% and a total flux of 15.4% toward the pool of fructose-6-phosphate, i.e., a fraction of 99% (10). According to the results, fructose-grown cells direct the available carbon from the pool of fructose-6-phosphate much more efficiently toward the oxidative part of the PPP than sucrose-grown cells.

For the flux analysis, it was assumed, on the basis of previous enzymatic measurements during growth of *C. glutamicum* (4), that fructose bisphosphatase is not active. The presence of an active fructose bisphosphatase, however, cannot be completely excluded, due to the different genetic background of the strain examined and the different cultivation conditions used. The isotopic labeling used for flux determination cannot differentiate between uptake of the fructose residue through PTS^{Man} and uptake by PTS^{Fru} with subsequent conversion via fructose bisphosphatase, so caution should perhaps be exercised with regard to these fluxes. It is clear, however, that 8.8% of the fructose unit of sucrose was channeled by one of these two routes. Previous enzymatic data showed no activity of fructose-1,6-bisphosphatase but significant activity of PTS^{Man} during growth of *C. glutamicum* on glucose or fructose (4). Due to this, the contribution of the mannose transporter appears very likely.

The contribution of glucose to trehalose synthesis determined by the simplified comparison of ^{13}C enrichment of the substrate and the trehalose monomer (76%) agreed fairly well with the actual flux value from the comprehensive approach utilizing metabolite and isotopomer modeling and a global fit of the data from three independent studies (87%). The simplified approach, however, strongly underestimated the fraction of the glucose monomer channeled into the PPP. The reason is the high reversibility of glucose-6-phosphate isomerase, which is fully taken into account by the comprehensive flux calculation but not by the simplified approach.

(iii) Pyruvate node. A high flux of 88.6% was channeled through pyruvate dehydrogenase toward the TCA cycle during lysine production by *C. glutamicum* on sucrose. The flux into the lysine pathway was 28.8%. The anaplerotic flux of 34.3% was relatively low, probably related to the low anabolic demand for oxaloacetate (Table 2). It was almost exclusively utilized for lysine formation, i.e., 84% of oxaloacetate supplied by anaplerosis was used for product formation, whereas only 16% was required for growth. Pyruvate is a highly connected node in the central metabolism of *C. glutamicum*. From this node carbon can be directed into pathways with different functions such as anabolism, energy formation, or lysine production. The distribution of carbon flux around the pyruvate node therefore reveals an important characteristic of the physiological state of the cells. As found for the flux partitioning between PPP and glycolysis, the fluxes around the pyruvate node also differed strongly depending on the carbon source. The pyruvate dehydrogenase flux on sucrose was much higher than that on glucose (70.9%) (10). Due to this, a substantially greater amount of carbon was channeled into the TCA cycle. The major reason for the increased pyruvate dehydrogenase flux is the reduced anabolic demand on sucrose, which leads to a lower withdrawal of carbon from the PPP and glycolysis. The different anabolic burdens on glucose and sucrose are also revealed by the flux through anaplerosis. On glucose, anabolism, consuming 32% of the oxaloacetate provided, played a more significant role as a pathway competing with lysine production for this important precursor.

(iv) TCA cycle. The entry reaction of the TCA cycle, citrate synthase, exhibited a relative flux of 78.2%. Obviously, a substantial amount of carbon was utilized for the formation of energy, leading to significant loss of carbon via carbon dioxide. Compared to that in glucose-grown cells, the activity of the TCA cycle was increased by about 25% (10). *C. glutamicum* growing on sucrose therefore produces about 1.5-fold more NADPH by isocitrate dehydrogenase than the same organism growing on glucose.

(v) NADPH metabolism. Flux quantification, providing accurate data for NADPH-supplying and -consuming reactions, allowed a detailed examination of the NAPDH metabolism. Based on the flux calculation, 190% NADPH was supplied by *C. glutamicum* during growth on sucrose. This was far more than the actual demand for lysine production (110%) and biomass formation (32%). The high NADPH production probably favored lysine formation on sucrose. The PPP and isocitrate dehydrogenase contributed similarly to overall NADPH formation. The apparent NADPH excess was statistically significant, as shown by the calculated 90% confidence intervals for the NADPH-supplying and -consuming reactions (Table 6).

The results point at one or several not yet identified reactions that reoxidize NAPDH in *C. glutamicum* during growth on sucrose. The ability to produce more NADPH than is actually required for growth and lysine production was also observed for *C. glutamicum* when glucose was the carbon source (25, 26). Thus, *C. glutamicum* shows an apparent NADPH excess on the two major carbon sources used in industrial production processes. This behavior might be a key feature of *C. glutamicum* and could explain why these two carbon sources result in excellent production characteristics for lysine. However, the use of glucose as a carbon source under conditions comparable to those in the present work resulted in only a slight apparent NADPH surplus (10), so that the difference between NAPDH supply and demand was even higher on sucrose. This is partly due to the lower anabolic NADPH demand, since the overall NAPDH supply is similar on the two substrates.

It should be noted that the relative contributions of the PPP and isocitrate dehydrogenase to NADPH supply differ between sucrose and glucose. Isocitrate dehydrogenase supplies 40% of the total NADPH on sucrose and 30% of that on glucose (10). On fructose, the relative NADPH supply by isocitrate dehydrogenase is 70%, even higher than that on sucrose. These differences provide an example of the metabolic flexibility of *C. glutamicum* to recruit different pathways for NADPH formation.

Conclusions. For the first time, metabolic fluxes in the central metabolism were determined for sucrose-grown *C. glutamicum* cells, providing detailed insight into molasses-based industrial production processes. The approach utilized allowed a precise estimation of flux, as indicated for various key pathways by the generally narrow 90% confidence intervals (Table 6). In summary, utilization of sucrose in *C. glutamicum* leads to a rather complex situation, with three different substrate uptake systems simultaneously involved and three different entry points into the metabolism. As the results show, ^{13}C flux analysis is a powerful approach for resolving fluxes linked to simultaneous uptake of different nutrients. From a biotechnological point of view, *C. glutamicum* ATCC 21526 cultured on sucrose revealed lysine production characteristics similar to those previously observed for cultivation on glucose. The use of sucrose allows a relatively high flux through the PPP combined with a generally low anabolic burden. Due to this, sucrose-grown *C. glutamicum* cells exhibit a high NADPH supply, which is required for anabolic purposes to a much lesser extent than on glucose. On sucrose, the ratio between NADPH utilized for lysine and NADPH required for biomass production is 3.4, much more favorable than the ratio of 1.7 on glucose (10).

Various investigations of *C. glutamicum* in the recent past have led to valuable suggestions concerning targets for the optimization of lysine production by this organism. These include, e.g., amplification of the flux through the PPP, amplification of the anaplerotic flux, or deletion of reactions withdrawing the lysine precursor oxaloacetate (24). An interesting target, not previously taken into account, emerges from the present study. On sucrose a relatively large amount of carbon was channeled into the TCA cycle and used for energy formation. *C. glutamicum* ATCC 21526, however, exhibits reduced growth during lysine production, so the energy produced is probably not needed (26). The relatively high TCA cycle flux is therefore not required for energetic purposes or for anabolic purposes. Thus, it simply leads to substantial loss of carbon as CO_2. A further drawback of the high TCA cycle flux is the fact that the energy surplus produced activates futile cycles for the regeneration of the ATP formed (26). These involve the recycling of C_4 metabolites of the TCA cycle into C_3 metabolites of glycolysis and are thus linked to the undesired consumption of the lysine precursor oxaloacetate (26). The remaining high TCA cycle flux on sucrose therefore is an interesting target to be approached by genetic engineers in order to optimize the strain investigated. Targeted decrease of the flux through the TCA cycle could reduce the still significant amount of carbon that is wasted by the decarboxylation reactions involved and direct it toward the formation of lysine. The same holds for the overflow metabolites glycerol and dihydroxyacetone.

REFERENCES

1. **Cocaign, M., C. Monnet, and N. D. Lindley.** 1993. Batch kinetics in *Corynebacterium glutamicum* during growth on various carbon substrates: use of substrate mixtures to localize metabolic bottlenecks. Appl. Microbiol. Biotechnol. **40:**526–530.
2. **Cocaign-Bousquet, M., and N. D. Lindley.** 1995. Pyruvate overflow and carbon flux within the central metabolic pathways of *Corynebacterium glutamicum* during growth on lactate. Enzyme Microbiol. Technol. **17:**260–267.
3. **Dominguez, H., and N. D. Lindley.** 1996. Complete sucrose metabolism requires fructose phosphotransferase activity in *Corynebacterium glutamicum* to ensure phosphorylation of liberated fructose. Appl. Environ. Microbiol. **62:**3878–3880.
4. **Dominguez, H., C. Rollin, A. Guyonvarch, J. L. Guerquin-Kern, M. Cocaign-Bousquet, and N. D. Lindley.** 1998. Carbon-flux distribution in the central metabolic pathways of *Corynebacterium glutamicum* during growth on fructose. Eur. J. Biochem. **254:**96–102.
5. **Fiechter, A., and F. K. Gmunder.** 1989. Metabolic control of glucose degradation in yeast and tumor cells. Adv. Biochem. Eng. Biotechnol. **39:**1–28.
6. **Gombert, A. K., M. Moreira dos Santos, B. Christensen, and J. Nielsen.** 2001. Network identification and flux quantification in the central metabolism of *Saccharomyces cerevisiae* under different conditions of glucose repression. J. Bacteriol. **183:**1441–1451.
7. **Ikeda, M., and R. Katsumata.** 1999. Hyperproduction of tryptophan by *Corynebacterium glutamicum* with the modified pentose phosphate pathway. Appl. Environ. Microbiol. **65:**2497–2502.
8. **Ikeda, M.** 2003. Amino acid production processes. Adv. Biochem. Eng. Biotechnol. **79:**1–36.
9. **Kiefer, P., E. Heinzle, and C. Wittmann.** 2002. Influence of glucose, fructose and sucrose on kinetics and stoichiometry of lysine production by *Corynebacterium glutamicum.* J. Ind. Microbiol. Biotechnol. **28:**338–343.
10. **Kiefer, P., E. Heinzle, O. Zelder, and C. Wittmann.** 2004. Comparative metabolic flux analysis of lysine-producing *Corynebacterium glutamicum* cultured on glucose or fructose. Appl. Environ. Microbiol. **70:**229–239.
11. **Pelechová, J., J. Smekal, V. Koura, J. Plachý, and V. Krumphanzl.** 1980. Biosynthesis of L-lysine in *Corynebacterium glutamicum* on sucrose, ethanol and acetic acid. Fol. Microbiol. **25:**341–346.
12. **Plachý, J.** 1975. The effect of medium composition on the production of valine by *Corynebacterium* 9366-EMS/184. Fol. Microbiol. **20:**346–350.
13. **Plachý, J., S. Ulbert, J. Pelechová, and V. Krumphanzl.** 1985. Fermentation production of L-homoserine by *Corynebacterium* sp. and its possible use in the preparation of threonine and lysine. Fol. Microbiol. **30:**485–492.
14. **Shiio, I., S. Sugimoto, and K. Kawamura.** 1990. Effects of carbon source sugars on the yield of amino acid production and sucrose metabolism in *Brevibacterium flavum.* Agric. Biol. Chem. **54:**1513–1519.
15. **Shimakata, T., and Y. Minatogawa.** 2000. Essential role of trehalose in the synthesis and subsequent metabolism of corynomycolic acid in *Corynebacterium matruchotii.* Arch. Biochem. Biophys. **380:**331–338.
16. **Stephanopoulos, G., A. A. Aristidou, and J. Nielsen.** 1998. Metabolic engineering. Academic Press, San Diego, Calif.
17. **Tangney, M., and W. J. Mitchell.** 2000. Analysis of a catabolic operon for sucrose transport and metabolism in *Clostridium acetobutylicum* ATCC 824. J. Mol. Microbiol. Biotechnol. **2:**71–80.
18. **Thompson, J., and B. M. Chassy.** 1981. Uptake and metabolism of sucrose by *Streptococcus lactis.* J. Bacteriol. **147:**543–551.
19. **Tzvetkov, M., C. Klopprogge, O. Zelder, and W. Liebl.** 2003. Genetic dissection of trehalose biosynthesis in *Corynebacterium glutamicum*: inactivation of trehalose production leads to impaired growth and an altered cell wall lipid composition. Microbiology **149:**1659–1673.
20. **Vallino, J. J., and G. Stephanopoulos.** 1993. Metabolic flux distributions in *Corynebacterium glutamicum* during growth and lysine overproduction. Biotechnol. Bioeng. **41:**633–646.
21. **van Winden, W. A., C. Wittmann, E. Heinzle, and J. J. Heijnen.** 2002.

Correcting mass isotopomer distributions for naturally occurring isotopes. Biotechnol. Bioeng. **80:**477–479.
22. **Wagner, E., F. Gotz, and R. Bruckner.** 1993. Cloning and characterization of the *scrA* gene encoding the sucrose-specific enzyme II of the phosphotransferase system from *Staphylococcus xylosus.* Mol. Gen. Genet. **241:**33–41.
23. **Wendisch, V. F., A. A. de Graaf, H. Sahm, and B. Eikmans.** 2000. Quantitative determination of metabolic fluxes during co-utilization of two carbon sources: comparative analyses with *Corynebacterium glutamicum* during growth on acetate and/or glucose. J. Bacteriol. **182:**3088–3096.
24. **Wittmann, C., and A. A. de Graaf.** 2004. Metabolic flux analysis in *Corynebacterium glutamicum*. *In* L. Eggeling and M. Bott (ed.), Handbook of *Corynebacterium glutamicum*, in press. CRC Press LLC, Boca Raton, Fla.
25. **Wittmann, C., and E. Heinzle.** 2001. Application of MALDI-TOF MS to lysine-producing *Corynebacterium glutamicum*: a novel approach for metabolic flux analysis. Eur. J. Biochem. **268:**2441–2455.
26. **Wittmann, C., and E. Heinzle.** 2002. Genealogy profiling through strain improvement by using metabolic network analysis: metabolic flux genealogy of several generations of lysine-producing corynebacteria. Appl. Environ. Microbiol. **68:**5843–5859.
27. **Wittmann, C., M. Hans, and E. Heinzle.** 2002. In vivo analysis of intracellular amino acid labelings by GC/MS. Anal. Biochem. **307:**379–382.
28. **Wittmann, C., H. M. Kim, and E. Heinzle.** 2004. Metabolic network analysis of lysine producing *Corynebacterium glutamicum* at a miniaturized scale. Biotechnol. Bioeng. **87:**1–6.
29. **Wolf, A., R. Kramer, and S. Morbach.** 2003. Three pathways for trehalose metabolism in *Corynebacterium glutamicum* ATCC 13032 and their significance in response to osmotic stress. Mol. Microbiol. **49:**1119–1134.
30. **Wurster, B., and F. Schneider.** 1970. Kinetics of glucose phosphate isomerase from yeast in vitro and its application to flux calculations for the fermentation pathway of anaerobic yeast cells. Hoppe-Seyler's Z. Physiol. Chem. **351:**961–966.